# Mechanosensory trichome cells evoke a mechanical stimuli–induced immune response in plants

Mamoru Matsumura[1,10], Mika Nomoto[1,2,10]*, Tomotaka Itaya[1,2], Yuri Aratani[3], Mizuki Iwamoto[4], Takakazu Matsuura[5], Yuki Hayashi[1], Toshinori Kinoshita[1,6], Izumi C Mori[5], Takamasa Suzuki[7], Shigeyuki Betsuyaku[4,8], Steven H Spoel[9], Masatsugu Toyota[3], Yasuomi Tada[1,2]*

[1]Division of Biological Science, Graduate School of Science, Nagoya University, Aichi, Japan.

[2]Center for Gene Research, Nagoya University, Aichi, Japan.

[3]Department of Biochemistry and Molecular Biology, Saitama University, Saitama, Japan.

[4]Graduate School of Life and Environmental Sciences, University of Tsukuba, Ibaraki, Japan.

[5]Institute of Plant Science and Resources (IPSR), Okayama University, Okayama, Japan.

[6]Institute of Transformative Bio-Molecules (WPI-ITbM), Nagoya University, Aichi, Japan.

[7]Department of Biological Chemistry, College of Bioscience and Biotechnology, Chubu University, Aich, Japan.

[8]Faculty of Life and Environmental Sciences Microbiology Research Center for Sustainability, University of Tsukuba, Ibaraki, Japan.

[9]Institute of Molecular Plant Sciences, School of Biological Sciences, University of Edinburgh, Edinburgh, UK.

[10]These authors contributed equally.

Lead contact

*Correspondence: nomoto@gene.nagoya-u.ac.jp (M.N.); ytada@gene.nagoya-u.ac.jp (Y.T.).

## Abstract

Perception of pathogen-derived ligands by corresponding host receptors is a pivotal strategy in eukaryotic innate immunity. In plants, this is complemented by circadian anticipation of infection timing, promoting basal resistance even in the absence of pathogen threat. Here, we report that trichomes, hair-like structures on the epidermis, directly sense external mechanical forces caused by raindrops to anticipate waterborne infections in *Arabidopsis thaliana*. Exposure of leaf surfaces to mechanical stimuli initiates the concentric propagation of intercellular calcium waves away from trichomes to induce defence-related genes. Propagating calcium waves enable effective immunity against pathogenic microbes through the calmodulin-binding transcription activator 3 (CAMTA3) and mitogen-activated protein kinases. We propose a novel layer of plant immunity in which trichomes function as mechanosensory cells to detect potential risks.

38 ## Introduction

39 Innate immunity is an evolutionarily conserved front line of defence across the plant and
40 animal kingdoms. In plants, pattern-recognition receptors (PRRs), such as leucine-rich repeat
41 receptor-like kinases (LRR-RLKs) and LRR receptor proteins (LRR-RPs), specifically
42 recognize microbe-associated molecular patterns (MAMPs) as non-self molecules, leading
43 to the activation of pattern-triggered immunity (PTI) to limit pathogen proliferation[1,2]. While
44 adapted pathogens have evolved virulence effectors that can circumvent PTI, plants also
45 deploy disease resistance (*R*) genes, primarily encoding nucleotide-binding LRR proteins,
46 which mount effector-triggered immunity (ETI)[3-5]. ETI often culminates in a hypersensitive
47 response as well as acute and localized cell death induced at the site of infection and
48 accompanied by profound transcriptional changes of defence-related genes to retard
49 pathogen growth[4,5]. These ligand-receptor systems are largely dependent on a transient
50 increase in intracellular calcium concentration ($[Ca^{2+}]_i$), followed by the initiation of
51 phosphorylation-dependent signalling cascades, including mitogen-activated protein kinases
52 (MAPKs) and calcium-dependent protein kinases, that orchestrate a complex transcriptional
53 network and the activity of immune mediators[6,7].

54 In addition to PTI and ETI, plant immunity can be induced periodically in the
55 absence of pathogen threat, a process that is under the control of the circadian clock and
56 driven by daily oscillations in humidity as well as light-dark cycles[8-10]. Such responses enable
57 plants to prepare for the potential increased risk of infection at the time when microbes are
58 anticipated to be most infectious. Therefore, the anticipation of potentially pathogenic
59 microorganisms through sensing of climatological changes on the one hand and their specific
60 detection on the other constitute two distinct layers of the plant immune system.

61 Among the climatological factors that affect the outcome of plant-microbe
62 interactions, rain is a major cause of devastating plant diseases, as fungal spores and bacteria
63 are spread through rain-dispersed aerosols or ballistic particles splashed from neighbouring
64 infected plants. In addition, raindrops contain plant pathogens, including *Pseudomonas*
65 *syringae* and *Xanthomonas campestris*, and negatively regulate stomatal closure, which
66 facilitates pathogen entry into leaf tissues[11-13]. High humidity, which is usually associated
67 with rain, enhances the effects of bacterial pathogen effectors, such as HopM1, and
68 establishes an aqueous apoplast for aggressive host colonization[14]. These findings suggest
69 that it would be beneficial for plants to recognize rain as an early risk factor for infectious
70 diseases.

71 How do plants respond to rain? Rain induces the expression of mechanosensitive
72 *TOUCH* (*TCH*) genes in plants[15]. Mechanostimulation may affect a variety of plant
73 physiological processes mediated by hormones such as auxin, ethylene, and gibberellin[16-19].
74 *Arabidopsis thaliana* seedlings exposed to rain-simulating water spray accumulate the
75 immune phytohormone jasmonic acid (JA) to promote the expression of JA-responsive
76 genes[20]. Thus, rain modulates both mechanotransduction and hormone-signalling pathways
77 that could affect the growth and development of plants as well as environmental responses.
78 However, the regulatory mechanisms underpinning the rain-activated signalling pathway
79 have not been fully elucidated.

80 Here, we report a novel layer of the plant immune system evoked by sensing
81 mechanostimulation of falling raindrops: trichomes, hair-like cells on the leaf surface,
82 function as mechanosensory cells that mount an effective immune response against both
83 biotrophic and necrotrophic pathogens. When trichomes are mechanically stimulated,
84 intercellular calcium waves are concentrically propagated away from them, and this is

85 followed by the activation of MAPKs and initiation of the calcium- and calmodulin-binding
86 transcription activator (CAMTA)-regulated immune response. We propose that plants
87 directly recognize rain as a risk factor and evoke a rapid immune response that substantially
88 contributes to early detection of, and protection from, potential pathogens.

89

## 90 Results and discussion

### 91 Rain and mechanical stimuli induce mechanosensitive genes involved in plant immunity

92 To investigate the effect of rain on transcriptional changes in *Arabidopsis* leaves, we
93 performed transcriptome deep sequencing (RNA-seq) of wild-type Columbia (Col-0)
94 *Arabidopsis* treated with artificial raindrops (Supplementary Fig. 1a; Methods). After
95 applying only 10 falling droplets, we detected the marked induction of 1,050 genes 15 min
96 after treatment (Supplementary Table 1). Gene Ontology (GO) analysis of these genes
97 revealed a striking enrichment in categories associated with plant immunity, as evidenced by
98 the expression of major immune regulators including *WRKY DNA-BINDING PROTEIN*
99 (*WRKY*) genes, *CALMODULIN BINDING PROTEIN 60-LIKE* g (*CBP60g*), *MYB DOMAIN*
100 *PROTEIN* (*MYB*) genes, *ETHYLENE RESPONSE FACTOR* (*ERF*) genes, and *MAP KINASE*
101 (*MPK*) genes[21,22] (Fig. 1a, Supplementary Table 1, Supplementary Table 2). The touch-
102 induced genes *TCH2* and *TCH4* were also highly upregulated in response to one falling
103 raindrop (falling) compared to a water droplet placed directly on the leaf surface (static)
104 (Supplementary Fig. 1b). These results suggested that mechanosensation is involved in
105 altering transcriptional activity.

106 To validate this hypothesis, we mechanically stimulated rosette leaves by gently
107 brushing them one to ten times along the main veins with a small paint brush (Supplementary
108 Fig. 1c; Methods) and analysed the expression profile of the immune regulator *WRKY33*,

109 which was responsive to raindrops. *WRKY33* expression was maximally induced 15 min after
110 brushing the leaves one to four times (Supplementary Fig. 1d). Next, we compared gene
111 expression patterns between leaves that were brushed once and those that received 10 falling
112 raindrops. Both raindrops and brushing strongly upregulated *TCH2*, *TCH4*, *WRKY33*,
113 *WRKY40*, *WRKY53*, *CBP60g*, *MYB51*, *ERF1*, and *JASMONATE-ZIM-DOMAIN PROTEIN*
114 *1* (*JAZ1*) expression [15,21,22] (Fig. 1b, c), suggesting that raindrops are likely recognized as a
115 mechanical stimulus.

116 Then, to comprehensively identify mechanosensitive genes, we performed an RNA-
117 seq analysis of leaves brushed once. We identified 1,241 genes that were significantly
118 induced 15 min after this treatment relative to control plants (Supplementary Table 3). These
119 mechanical stimuli (MS)-induced genes were primarily categorized as plant immune
120 responses, such as response to chitin, defence response, and immune system response (Fig.
121 1d, Supplementary Table 4). We found that 87.3% of raindrop-induced genes and 73.9% of
122 MS-induced genes overlapped (Fig. 1e): this set of 917 genes expressed upon both treatments
123 was enriched in GO categories associated with stress responses (Supplementary Fig. 1e).
124 Furthermore, the expression levels of these 917 genes, including major immune regulators,
125 were strongly positively correlated between the two treatments (Pearson correlation
126 coefficient $r = 0.917$) (Fig. 1f). These transcriptome analyses indicated that falling raindrops
127 stimulate the expression of mechanosensitive genes involved in environmental stress
128 responses, including plant immunity.

129

130 **Rain and MS rapidly activate plant immune responses**

131 To further characterize raindrop-induced genes, we conducted a comparative analysis with
132 published transcriptome datasets. Many raindrop- and MS-induced genes were also

133 expressed during major plant immune responses, such as those triggered by the immune
134 phytohormones salicylic acid (SA), which is effective against biotrophic pathogens (21%;
135 193/917 genes), and JA, which mounts immune responses to necrotrophic pathogens (11.8%;
136 108/917 genes); the bacterial-derived peptide flg22, which activates PTI (37%; 339/917
137 genes); and the bacterial pathogen *Pseudomonas syringae* pathovar *maculicola* ES4326 (*Psm*
138 ES4326) (25.8%; 237/917 genes)[1,2,23-25] (Fig. 2a, b). In total, 58.6% (537/917 genes) of
139 raindrop- and MS-induced genes overlapped with those induced in response to different
140 immune elicitors, suggesting that raindrops activate mechanosensitive immune responses.

141 Since stress-responsive gene expression is either positively or negatively regulated
142 by phytohormones, we determined the changes in the accumulation levels of six
143 phytohormones [SA, JA, JA-isoleucine (JA-Ile), abscisic acid (ABA), gibberellic acid 4
144 ($GA_4$), and indole-3-acetic acid (IAA)] in leaves treated with 10 falling droplets and in those
145 brushed once. No significant changes in the levels of the phytohormones, except JA and JA-
146 Ile, were observed 5 min after treatment (Fig. 2c), consistent with the previous report that
147 water spray induces JA-mediated transcriptional changes[20]. The slight increase in JA and JA-
148 Ile could explain the observation that only 11.8% of raindrop- and MS-induced genes are JA-
149 responsive (Fig. 2a). Although 21% of raindrop- and MS-induced genes overlap with SA-
150 responsive genes (Fig. 2a), SA levels were not significantly increased in response to
151 raindrops and MS (Fig. 2c). Therefore, most mechanosensitive genes, whose expression is
152 induced 5 min after treatment with raindrops, are presumably regulated independently of
153 phytohormonal responses. A previous report demonstrated that GA accumulation is reduced
154 by "bending" leaves twice per day for 2 weeks[19]. Here, significant changes in GA levels were
155 not detected upon transient application of raindrops or MS (data not shown). These results
156 indicated that plants differentially respond to MS depending on their intensity and duration.

157 Activation of MAPKs is one of the earliest cellular events and a hallmark of plant
158 immune responses. In particular, PRRs promptly activate a phosphorylation cascade
159 involving MPK3 and MPK6 in response to MAMPs, whereby the downstream immune
160 components of PTI are phosphorylated to promote transcriptional reprogramming[1,6,7,26].
161 Because 37% of raindrop- and MS-induced genes were also upregulated by flg22 treatment
162 (Fig. 2a), we examined whether a MAPK cascade is activated in responses to raindrops and
163 MS by immunoblot analysis with the anti-p44/p42 antibody, which detects phosphorylated
164 MPK3/MPK6[27,28]. Upon treatment of rosette leaves with 4 falling raindrops or MS (1
165 brushing), phosphorylation of MPK3/MPK6 was induced within 3 min and remained high
166 for 10 min after each treatment (Fig. 2d, e), indicating that MPK3/MPK6 activation precedes
167 the expression of mechanosensitive genes detected 10 min after MS application
168 (Supplementary Fig. 1d). The kinetics of MS-activated MPK3/MPK6 were reminiscent of
169 those observed upon activation of the PRR protein FLS2 and its coreceptor BRI1-
170 ASSOCIATED RECEPTOR KINASE 1 (BAK1), which are responsible for recognition of
171 the bacterial flg22 epitope[1,26]. Wild-type, *fls2*, and *bak1* mutant plants displayed comparable
172 levels of phosphorylated MPK3/MPK6 in response to MS (Fig. 2f), however, suggesting that
173 FLS2 and BAK1 are not positively involved in raindrop-elicited mechanotransduction.

174 We then performed a comparative analysis of raindrop- and MS-induced genes
175 against published transcriptome datasets describing the specific and conditional activation of
176 MPK3/MPK6 in transgenic *Arabidopsis* plants carrying a constitutively active variant of
177 tobacco (*Nicotiana tabacum*) *MAP KINASE Cab 2* (*NtMEK2*) under the control of the
178 dexamethasone-inducible promoter[28]. Approximately 27.5% (252/917 genes) of both
179 raindrop- and MS-induced genes were upregulated by MPK3/MPK6[28] (Supplementary Fig.
180 2a, Supplementary Table 5), and these upregulated genes were highly enriched in categories

181 associated with plant immunity (Supplementary Fig. 2b, Supplementary Table 6), suggesting
182 that MAPKs play a critical role in mechanotransduction.

183

184 **Rain and MS confer resistance to both biotrophic and necrotrophic pathogens**

185 We then investigated whether raindrops and MS confer resistance to pathogenic microbes.
186 Raindrops containing the spores of the necrotrophic pathogen *Alternaria brassicicola* Ryo-1
187 were placed on fully expanded leaves after pretreatment with raindrops or MS for 3 h at an
188 interval of 15 min. Both stimuli significantly suppressed lesion development compared to
189 control plants without pretreatment (Fig. 2g, h). Pretreatment of leaves with MS for 3 h also
190 efficiently protected plants from infection with the biotrophic pathogen *Psm* ES4326 (Fig.
191 2i). These results confirmed that mechanostimulation induces a PTI-like response to confer
192 a broad spectrum of resistance to both biotrophic and necrotrophic pathogens, as MS activate
193 immune MAPKs and upregulate a large subset of flg22-induced genes. In support of this
194 argument, exposure to the fungal cell wall, chitin, also upregulated 42.1% (386/917 genes)
195 of raindrop-induced genes (Supplementary Fig. 2c).

196

197 **Mechanosensitive genes are regulated by calmodulin-binding transcription activator 3**

198 To dissect rain-induced mechanotransduction, we searched for a conserved *cis*-regulatory
199 element in the promoter sequences of mechanosensitive genes. From an unbiased promoter
200 analysis of the top 300 genes among 917 differentially expressed genes, we obtained the
201 highest enrichment for the CGCG box (CGCGT or CGTGT), which is recognized by
202 calmodulin (CaM)-binding transcription activators (CAMTAs) that are conserved from
203 plants to mammals[29-33] (Fig. 3a). The *Arabidopsis* transcription factor CAMTA3 (also named

204 SIGNAL RESPONSIVE1 [SR1]) is a negative regulator of plant immunity because *camta3*
205 null mutants exhibit constitutive expression of defence-related genes and enhanced resistance
206 to virulent *P. syringae* infection[34,35]. CAMTA transcription factors possess a CaM-binding
207 (CaMB) domain and an IQ domain to which CaM binds in a calcium-dependent manner to
208 negate their function (Supplementary Fig. 3a). Mutation of the IQ domain, such as in
209 CAMTA3$^{A855V}$, suppresses the constitutive expression of defence-related genes seen in the
210 *camta2 camta3* double mutant when expressed in this background but is no longer regulated
211 by calcium-mediated responses[36,37]. In agreement with our promoter analysis, 28.7% of
212 constitutively upregulated genes (309/1,075 genes) in the *camta1 camta2 camta3* triple
213 mutant overlapped with raindrop- and MS-induced genes detected in wild-type plants[38]
214 (Supplementary Fig. 3b, Supplementary Table 7). Upon application of raindrops and MS,
215 *WRKY33* and *CBP60g* transcript levels were significantly reduced in plants expressing the
216 *CAMTA3$^{A855V}$* variant compared to a *CAMTA3-GFP* transgenic line expressing a transgene
217 that complemented the phenotype of the *camta2 camta3* mutant (Fig. 3b, c), suggesting that
218 CAMTA3 is involved in mechanotransduction.

219 To confirm whether CAMTA3 directly targets mechanosensitive genes, we
220 investigated the genome-wide distribution of CAMTA3-binding sites by chromatin
221 immunoprecipitation followed by deep sequencing (ChIP-seq) using *CAMTA3$^{A855V}$-GFP*
222 plants, as the mutant protein stably represses the transcription of CAMTA3-regulated genes.
223 With the aid of model-based analysis of ChIP-seq (MACS2) software, we identified 2,641
224 and 2,728 CAMTA3-binding genes, respectively, in two replicates ($P < 0.05$); about 40% of
225 these peaks are located in the promoter regions and another 30% in gene bodies
226 (Supplementary Fig. 3c, Supplementary Table 8). The overlap between the two replicates
227 highlighted 2,011 CAMTA3-targeted genes that included 272 raindrop- and 297 MS-induced

228 genes such as *TCH2*, *TCH4*, and *CBP60g* (Fig. 3d), consistent with our hypothesis that
229 CAMTA3 regulates the transcription of mechanosensitive genes.

230 To validate the results from the promoter analysis of mechanosensitive genes, we
231 next investigated specific DNA sequences to which CAMTA3 selectively binds by analysing
232 CAMTA3-binding peaks by Multiple EM for Motif Elicitation (MEME)-ChIP (Methods).
233 We again identified the CGCG box (CGCGT or CGTGT) as the motif with the highest
234 enrichment score ($3.4 \times 10^{-44}$) (Fig. 3e). The subsequent visualization of ChIP-seq profiles
235 via the Integrative Genomics Viewer (IGV)[39] demonstrated that CAMTA3 is primarily
236 enriched at the CGCG boxes of mechanosensitive genes, including *TCH2*, *TCH4*, *CAM2*,
237 *CBP60g*, *CALMODULIN LIKE 23* (*CML23*), and *WRKY40* (Fig. 3f). GO analysis on 314
238 CAMTA-targeted genes (Fig. 3d, shown in red) to define the biological functions of these
239 genes showed a significant enrichment in categories related to immune and environmental
240 responses (Supplementary Fig. 3d, e). We thus investigated whether CAMTA3 is required
241 for the immune responses. *camta2 camta3 CAMTA3-GFP* transgenic plants effectively
242 mounted an enhanced disease resistance against *P. syringae* in response to MS, while *camta2*
243 *camta3 CAMTA3*$^{A855V}$*-GFP* plants were significantly compromised in resistance (Fig. 3g).
244 These results demonstrate that CAMTA3 negatively regulates the plant immune responses
245 by binding to the CGCG box in raindrop- and MS-induced gene promoters and represses the
246 expression of these genes.

247 Since mechanostimulation rapidly activates MPK3/MPK6 (Fig. 2d, e), we
248 investigated whether CAMTA3 mediates the activation of these MPKs. Using *camta2*
249 *camta3 CAMTA3-GFP* and *camta2 camta3 CAMTA3*$^{A855V}$*-GFP*, we detected the
250 phosphorylation of MPK3/MPK6 independently of CAMTA3 activity (Supplementary Fig.
251 3f). In addition, the calcium ionophore A23187 clearly induced the phosphorylation of MPK3

252 and MPK6 (Supplementary Fig. 3g). These results suggested that the mechanotransduction
253 initiated by raindrops and MS may cause a $Ca^{2+}$ influx that negates the repressive effect of
254 CAMTA3 and concomitantly activates the MAPK cascade, as previously proposed[26].

255

256 **MS initiates intercellular calcium waves concentrically away from trichomes**

257 To visualize how mechanostimulation induces the expression of immune genes *in planta*, we
258 generated *Arabidopsis* transgenic lines with the promoter sequences of *WRKY33* and
259 *CBP60g* driving the expression of nucleus-targeted enhanced *YELLOW FLUORESCENT*
260 *PROTEIN* (*YFP-NLS*) (*WRKY33pro:EYFP-NLS* and *CBP60gpro:EYFP-NLS*). *WRKY33*
261 expression is regulated by both MPK3/MPK6 and CAMTA3 (Supplementary Table 5,
262 Supplementary Table 8), while *CBP60g* is not mediated by MPK3/MPK6 (Supplementary
263 Table 5). When half leaves were gently brushed (Supplementary Fig. 1c), we detected YFP
264 fluorescence in the *WRKY33pro:EYFP-NLS* and *CBP60gpro:EYFP-NLS* transgenic lines as
265 localized, clustered groups of cells only in the brushed half (Fig. 4a, Supplementary Fig. 4a).
266 Closer inspection of the stimulated regions revealed that both genes were induced in cells
267 surrounding trichomes, hair-like structures projecting outward from the epidermal surface
268 (Fig. 4b, c, Supplementary Fig. 4b, c).

269 Trichomes function as chemical and physical barriers against insect feeding and are
270 likely involved in drought tolerance and protection against ultraviolet irradiation[40,41].
271 Mechanostimulation of a single trichome induces $Ca^{2+}$ oscillations within the proximal skirt
272 cells that surround the base of trichomes[42], suggesting that the mechanical force could be
273 focused on only skirt cells (Supplementary Fig. 5). However, since mechanostimulation by
274 raindrops and MS confers resistance to pathogens in whole leaves, we hypothesized that
275 trichomes activate a $Ca^{2+}$ signal in a large area of leaves, as shown in Figure 4a.

276 To visualize changes in cytosolic $Ca^{2+}$ concentrations ($[Ca^{2+}]_{cyt}$) induced by MS on
277 the leaf surface, we used transgenic *Arabidopsis* expressing the GFP-based $[Ca^{2+}]_{cyt}$ indicator
278 GCaMP3[43,44]. Leaf brushing induced a marked increase of $[Ca^{2+}]_{cyt}$ in the surrounding leaf
279 area of trichomes 1 min after stimulation (Fig. 4d, Supplementary Video 1). Flicking a single
280 trichome with a silver chloride wire triggered an intercellular calcium wave that propagated
281 concentrically away from the trichome and surrounding skirt cells at a speed of 1.0 μm/s (Fig.
282 4e, f, Supplementary Video 2). This pattern showed striking consistency with the area of
283 induction observed with the *WRKY33pro:EYFP-NLS* and *CBP60gpro:EYFP-NLS* reporters
284 (Fig. 4a, b; Supplementary Fig. 4a, b). The base of trichomes exhibited a rapid and transient
285 increase in $[Ca^{2+}]_{cyt}$ before the concentric propagation of calcium waves was initiated (Fig.
286 4g, Supplementary Video 3).

287

288 **Trichomes are mechanosensory cells activating plant immunity**

289 To investigate the possible involvement of trichomes in mechanosensation in *Arabidopsis*
290 leaves and activation of the immune response, we observed calcium waves using the
291 knockout mutant of *GLABROUS1* (*GL1*)[45], which lacks trichomes. The *gl1* mutant exhibits
292 effective basal resistance comparable to that of wild-type Col-0 plants[46], and its local
293 resistance to *Psm* ES4326 and *A. brassicicola* Ryo-1 is similar to the levels of Col-0 plants
294 (Supplementary Fig. 6). The mechanostimulation-induced propagation of concentric calcium
295 waves was compromised in the *gl1* mutant (Fig. 5a, b), confirming that trichomes are true
296 MS sensors and initiate calcium waves (Supplementary Videos 4, 5). Furthermore,
297 approximately 70.5% of mechanosensitive genes were expressed in a trichome-dependent
298 manner (Fig. 5c, Supplementary Fig. 7a, Supplementary Table 9), and transcript levels of 18
299 representative mechanosensitive immune genes were markedly lower at all time points in the

300 *gl1* mutant than they were in the wild type in RNA-seq analysis of leaves brushed 4 times
301 (Fig. 5d), suggesting that trichomes serve as the main sensor of MS. Similarly, compared to
302 wild-type plants, the transcription of raindrop-induced *WRKY33*, *WRKY40*, and *CBP60g*, as
303 well as the activation of MPK3/MPK6 by MS, was also significantly reduced in the *gl1*
304 mutant (Fig. 5e, f, Supplementary Fig. 7b). Moreover, MS-induced resistance against *Psm*
305 ES4326 infection was abrogated in the *gl1* mutant (Fig. 5g). As with *Psm* ES4326, the
306 application of MS to wild-type plants prior to inoculation with *A. brassicicola* significantly
307 limited lesion development, whereas the *gl1* mutant did not show enhanced disease resistance
308 in response to MS (Fig. 5h).

309 Our work highlights a novel layer of plant immunity that is triggered by an
310 unexpected function of trichomes as mechanosensory cells. When trichomes are
311 mechanically stimulated, intercellular calcium waves are concentrically propagated away
312 from the trichomes, followed by the activation of CAMTA3-dependent immune responses
313 (Fig. 6). Rapid phosphorylation of MAPKs also is a prerequisite for mechanosensitive gene
314 expression, as MPK3/MPK6 mediate the phosphorylation of mechanosensitive WRKY33 for
315 its activation[47,48]. This notion is supported by the finding that the expression of 252 genes
316 among 917 raindrop- and MS-induced genes is regulated by MPK3/MPK6 (Supplementary
317 Fig. 2a), and their promoter sequences possess the W-box (TTGACC) for WRKYs as the
318 most enriched *cis*-regulatory elements (Supplementary Fig. 8). The molecular mechanism by
319 which calcium mediates the activation of MPK3/MPK6 has yet to be elucidated.

320 Mechanostimulation by repeatedly bending leaves confers resistance to the
321 necrotrophic pathogen *Botrytis cinerea* via JA accumulation[49]. In addition, a subset of JA-
322 responsive genes upregulated by water spray is mediated by MYC2/MYC3/MYC4
323 transcription factors[20]. These observations strongly indicate that mechanosensation causes

324 profound JA-dependent changes in gene transcription, promoting plant immune responses to
325 necrotrophic pathogens. The JA- and MYC-dependent pathway does not play a major role in
326 the expression of mechanosensitive *TCH* genes, however, indicating that
327 mechanotransduction is regulated by other signaling pathways. Our work demonstrated that
328 raindrops and MS only partially activate the JA signal but rather strongly induce a PTI-like
329 response via the $Ca^{2+}$- and CAMTA3-dependent pathway, which is highly effective against
330 both necrotrophs and biotrophs (Fig. 2g-i). Because rain disseminates diverse pathogens with
331 different parasitic strategies, including fungi, bacteria, and virus[50,51], it is highly reasonable
332 that plants perceive raindrops as a risk factor and activate broad-spectrum resistance.

333 Plants possess mechanosensory cells with a variety of functions, such as flower
334 antennas of *Catasetum* species for pollination, tentacles of *Drosera rotundifolia* for insect
335 trapping, root hairs of *Arabidopsis* for water tracking, and red cells of *Mimosa pudica* for
336 evading herbivores[52]. The carnivorous Venus flytrap (*Dionaea muscipula*) captures insects
337 by sensing mechanostimulation via sensory hairs on leaf lobes[53]. To monitor diverse MS
338 applied to plants, several sensing mechanisms have been proposed that include the detection
339 of cell wall components, distortion of the plasma membrane, and the displacement of the
340 plasma membrane against the cell wall[54]. In all these systems, a transient increase in $[Ca^{2+}]_{cyt}$
341 is thought to play a pivotal role in short- and long-term responses. Indeed, two successive
342 stimulations of sensory hairs of the flytrap are required to meet the threshold of $[Ca^{2+}]_{cyt}$ for
343 rapid closure of the leaf blade[53,55]. As the trichome on the leaf surface is widely conserved
344 among many land plants, there may be a common and novel intercellular network of cell-cell
345 communication that initiates calcium waves for activating immune responses.
346

347 **Contact for reagents and subject details**

348 Further information and requests for reagents may be directed to and will be fulfilled by the
349 corresponding authors Yasuomi Tada (ytada@gene.nagoya-u.ac.jp) and Mika Nomoto
350 (nomoto@gene.nagoya-u.ac.jp).

351 **Experimental model and subject details**

352 **Plants**

353 *Arabidopsis thaliana* accession Columbia-0 (Col-0) was the background for all plants used
354 in this study. *WRKY33pro:EYFP-NLS* (Col-0) and *CBP60gpro:EYFP-NLS* (Col-0) were
355 generated as previously described[56]. *35Spro:GCaMP3* (Col-0), *gl1* [Col(*gl1*)], *camta2*
356 *camta3 CAMTA3pro:CAMTA3-GFP*, and *camta2 camta3 CAMTA3pro:CAMTA3*$^{A855V}$*-GFP*
357 were previously reported[36,38]. The *Arabidopsis* mutants *fls2* (SALK_093905) and *bak1-3*
358 (SALK_034523) were obtained from the Arabidopsis Biological Resource Center (ABRC).
359 *35Spro:GCaMP3* was introduced into the *gl1* mutant background by crossing. The selection
360 of homozygous lines was performed by genotyping using primers listed in Supplementary
361 Table 10. Plants were grown on soil (peat moss; Super Mix A and vermiculite mixed 1:1) at
362 22°C under diurnal conditions (16-h-light/8-h-dark cycles) with 50-70% relative humidity.
363 *WRKY33pro:EYFP-NLS* (Col-0) and *CBP60gpro:EYFP-NLS* (Col-0) were sown on soil and
364 grown in a growth room at 23°C in constant light as previously described[56]. *35Spro*:*GCaMP3*
365 (Col-0) and *35Spro*:*GCaMP3* (*gl1*) were grown on Murashige and Skoog (MS) plates [1%
366 (w/v) sucrose, 0.01% (w/v) myoinositol, 0.05% (w/v) MES, and 0.5% (w/v) gellan gum pH
367 5.8] as previously described[44,57].

368 **Artificial raindrop treatment**

369 Reverse osmosis (RO) water was kept in a 500 mL beaker until the water temperature reached
370 room temperature (22°C). A transfusion set (NIPRO Infusion Set TI-U250P, Nipro, Osaka,
371 Japan) was installed on a steel stand with the beaker at a height of 1.2 m (H-type Stand I3,
372 As One, Osaka, Japan) and was adjusted to release 13 μL water droplets (Supplementary Fig.
373 1a). In this setting, the applied mechanical energy to the leaf surface is equivalent to one in
374 which 5.8 μL of raindrops reach a terminal velocity of 6.96 m/s[58]. This size raindrop is
375 frequently observed in nature; thus, the impact of simulated rain is comparable with that of
376 true rain[58]. The adaxial side of leaves from 4-week-old plants was treated with 10 droplets
377 for RNA-seq, and 1, 4 or 10 droplets for quantitative RT-PCR (RT-qPCR). The adaxial side
378 of leaves from 4-week-old plants was treated with one falling or static droplet
379 (Supplementary Fig. 1b). Sample leaves were collected 15 min after treatment and stored at
380 -80 °C until use.

381 **Brush treatment**

382 The adaxial side of leaves from 4-week-old plants was brushed once for RNA-seq and 4 for
383 RT-qPCR along the main veins at an angle of 30-40° (KOWA nero nylon drawing pen flat
384 12, Kowa, Aichi, Japan) (Supplementary Fig. 1c). Sample leaves were collected 15-, 30- and
385 60 min after treatment for RNA-seq and 15 min for RT-qPCR, and stored at -80°C until use.

386 **RNA-seq library construction**

387 Total RNA was extracted from 80-100 mg frozen samples using Sepasol-RNA I Super G
388 (Nacalai Tesque, Kyoto, Japan) and the TURBO DNase free kit (Thermo Fisher Scientific,
389 IL, USA) according to the manufacturers' protocols. Total RNA was further purified with
390 the RNeasy RNA Isolation Kit (QIAGEN, Hilden, Germany) and assessed for quality and
391 quantity with a Nanodrop spectrophotometer (Thermo Fisher Scientific). We used 1 μg total

392 RNA for mRNA purification with NEBNext Oligo d(T)$_{25}$ (NEBNext poly(A) mRNA
393 Magnetic Isolation Module; New England Biolabs, MA, USA), followed by first-strand
394 cDNA synthesis with the NEBNext Ultra DNA Library Prep Kit for Illumina (New England
395 Biolabs) and NEBNext Multiplex Oligo for Illumina (New England Biolabs) according to
396 the manufacturer's protocols. For the analysis of raindrop- and MS-induced gene expression,
397 the amount of cDNA was determined on an Agilent 4150 TapeStation System (Agilent, CA,
398 USA). cDNA libraries were sequenced as single-end reads for 81 nucleotides on an Illumina
399 Nextseq 550 (Illumina, CA, USA). The reads were mapped to the *Arabidopsis thaliana*
400 reference genome (TAIR10, http://www.arabidopsis.org/) online (BaseSpace, Illumina,
401 https://basespace.illumina.com/). Pairwise comparisons between samples were performed
402 with the EdgeR[59] package on the web (Degust, https://degust.erc.monash.edu/). For the
403 comparative analysis of differentially expressed genes between leaves in the *gl1* mutant and
404 Col-0, the amount of cDNA was determined by the QuantiFluor dsDNA System (Promega,
405 WI, USA). cDNA libraries were sequenced as single-end reads for 36 nucleotides on an
406 Illumina Nextseq 500 (Illumina). The reads were mapped to the *Arabidopsis thaliana*
407 reference genome (TAIR10) via Bowtie[60] with the options "--all --best --strata". Pairwise
408 comparisons between samples were performed with the EdgeR package in the R program[59].
409 Enrichment of GO categories for biological processes was determined using BiNGO
410 (http://www.psb.ugent.be/cbd/papers/BiNGO/Home.html) ($P < 0.05$)[61].

411 **Re-analysis of immune-related transcriptome datasets**

412 We used the following public transcriptome datasets for the comparative analysis with the
413 RNA-seq data obtained in this study: 10-day-old *Arabidopsis* seedlings treated with 1 μM
414 flg22 (Array Express; E-NASC-76)[62], 8-day-old *Arabidopsis* seedlings treated with 40 μM
415 chitin (Gene Expression Omnibus GSE74955), leaves from 4-week-old *Arabidopsis* plants

416 inoculated with *Pseudomonas syringae* pv. *maculicola* (*Psm*) ES4326 (24 h post inoculation)
417 (GSE18978), 2-week-old *Arabidopsis* seedlings treated with 0.5 mM SA or 50 μM JA (DNA
418 Data Bank of Japan DRA003119), 12-day-old *Arabidopsis GVG-NtMEK2*$^{DD}$ seedlings
419 treated with 2 μM DEX for 0 and 6 h (NCBI Sequence Read Archive SRP111959), and 4-
420 week-old *Arabidopsis camta1 camta2 camta3* triple mutant (GSE43818). The overlaps
421 between differentially expressed genes in each transcriptome dataset were evaluated as Venn
422 diagrams (http://bioinformatics.psb.ugent.be/webtools/Venn/).

423 **RT-qPCR**

424 Total RNA was extracted from 30-40 mg leaf tissues with Sepasol-RNA I Super G and the
425 TURBO DNase free kit (Thermo Fisher Scientific) according to the manufacturer's protocols,
426 followed by reverse transcription with the PrimeScript RT reagent kit (Takara Bio, Shiga,
427 Japan) using oligo dT primers. RT-qPCR was performed on the first-strand cDNAs diluted
428 20-fold in water using KAPA SYBR FAST qPCR Master Mix (2x) kit (Roche, Basel,
429 Switzerland) and gene-specific primers in a LightCycler 96 (Roche). Primer sequences are
430 listed in Supplementary Table 10.

431 **Quantification of plant hormones**

432 The adaxial side of leaves from 4-week-old plants was treated with 10 raindrops (raindrop),
433 brushed once (MS), and cut (wounding). Sample leaves (0.07-0.1 g) were collected 5 min
434 after treatment and stored at -80°C until use. SA, JA, JA-Ile, ABA, IAA, and $GA_4$ were
435 extracted and purified by solid-phase extraction. The contents of these hormones were
436 quantified using liquid chromatography-electrospray tandem mass spectrometry (LC-ESI-
437 MS/MS) (triple quadrupole mass spectrometer with 1260 high-performance LC, G6410B;
438 Agilent Technologies Inc., CA, USA), as previously reported[63].

439 **ChIP assay**

440 Approximately 0.7 g of 2-week-old *camta2 camta3 CAMTA3pro:CAMTA3*$^{A855V}$*-GFP*
441 seedlings was fixed in 25 mL 1% formaldehyde under vacuum for three cycles of 2 min ON/2
442 min OFF using an aspirator (SIBATA, Tokyo, Japan). Subsequently, 1.5 mL of 2 M glycine
443 was added to quench the cross-linking reaction under vacuum for 2 min. The samples were
444 then washed with 50 mL double-distilled water and stored at -80°C until use. Frozen samples
445 were ground to a fine powder with a mortar and pestle in liquid nitrogen and dissolved in 2.5
446 mL nuclei extraction buffer (10 mM Tris-HCl pH 8.0, 0.25 M sucrose, 10 mM $MgCl_2$, 40
447 mM β-mercaptoethanol, protease inhibitor cocktail)[64]. Samples were filtered through two
448 layers of Miracloth (Calbiochem, CA, USA) and centrifuged at 17,700 g at 4°C for 5 min.
449 The pellets were resuspended in 75 µL nuclei lysis buffer [50 mM Tris-HCl pH 8.0, 10 mM
450 EDTA, 1% (w/v) SDS]. After incubation first at room temperature for 20 min and then on
451 ice for 10 min, the samples were mixed with 225 µL ChIP dilution buffer without Triton
452 [16.7 mM Tris-HCl pH 8.0, 167 mM NaCl, 1.2 mM EDTA, 0.01% (w/v) SDS]. Chromatin
453 samples were sonicated for 35 cycles of 30 sec ON/30 sec OFF using a Bioruptor UCW-201
454 (Cosmo Bio, Tokyo, Japan) to produce DNA fragments, followed by the addition of 375 µL
455 ChIP dilution buffer without Triton, 200 µL ChIP dilution buffer with Triton [16.7 mM Tris-
456 HCl pH 8.0, 167 mM NaCl, 1.2 mM EDTA, 0.01% (w/v) SDS, 1.1% (w/v) Triton X-100],
457 and 35 µL 20% (w/v) Triton X-100. After centrifugation at 17,700 g at 4°C for 5 min, 900
458 µL solubilized sample was split into two 2.0 mL PROKEEP low-protein-binding tubes
459 (Watson Bio Lab USA, CA, USA) and incubated with 0.75 µL anti-GFP antibody (for
460 immunoprecipitation [IP]) (ab290; Abcam, Cambridge, UK) or Rabbit IgG-Isotype Control
461 (Input) (ab37415; Abcam) for 4.5 h with gentle rocking, and an 18 µL aliquot was used as
462 the input control. Then, samples from *camta2 camta3 CAMTA3pro:CAMTA3*$^{A855V}$*-GFP* were
463 mixed with 50 µL of a slurry of Protein A agarose beads (Upstate, Darmstadt, Germany) and

464 incubated at 4°C for 1 h with gentle rocking. Beads were washed twice with 1 mL low-salt
465 wash buffer [20 mM Tris-HCl pH 8.0, 150 mM NaCl, 2 mM EDTA, 0.1% (w/v) SDS, 1%
466 (w/v) Triton X-100], twice with 1 mL high-salt wash buffer [20 mM Tris-HCl pH 8.0, 500
467 mM NaCl, 2 mM EDTA, 0.1% (w/v) SDS, 1% (w/v) Triton X-100], twice with 1 mL LiCl
468 wash buffer [10 mM Tris-HCl pH 8.0, 0.25 M LiCl, 1 mM EDTA, 1% (w/v) sodium
469 deoxycholate, 1% (w/v) Nonidet P-40], and twice with 1 mL TE buffer [10 mM Tris-HCl pH
470 8.0, 1 mM EDTA]. After washing, beads were resuspended in 100 μL elution buffer [1%
471 (w/v) SDS, 0.1 M $NaHCO_3$] and incubated at 65°C for 30 min. For the input controls, 41.1
472 μL TE buffer, 8.7 μL 10% (w/v) SDS, and 21 μL elution buffer were added to 18 μL of each
473 solubilized sample. Both supernatant and input samples were mixed with 4 μL of 5 M NaCl
474 and incubated at 65°C overnight to reverse the cross-linking, followed by digestion with 1
475 μL Proteinase K (20 mg/ml) (Invitrogen, CA, USA) at 37°C for 1 h. ChIP samples were
476 mixed with 500 μL Buffer NTB and purified using the PCR clean-up gel extraction kit
477 following the manufacturer's instructions (MACHEREY-NAGEL, Düren, Germany).

478 **ChIP-seq library construction**

479 ChIP-seq libraries for the input and two biological replicates were constructed from 2 ng
480 purified DNA samples with the NEB Ultra II DNA Library Prep Kit for Illumina (New
481 England Biolabs) according to the manufacturer's instructions. The amount of DNA was
482 determined on an Agilent 4150 TapeStation System (Agilent). All ChIP-seq libraries were
483 sequenced as 81-nucleotide single-end reads using an Illumina NextSeq 550 system.

484 **Analysis of ChIP-seq**

485 Reads were mapped to the *Arabidopsis thaliana* reference genome (TAIR10,
486 http://www.arabidopsis.org/) using Bowtie2 with default parameters[60]. The Sequence

487 Alignment/Map (SAM) file generated by Bowtie2 was converted to a Binary Alignment/Map
488 (BAM) format file by SAMtools[65]. To visualize mapped reads, Tiled Data Files (TDF) file
489 were generated from each BAM file using the igvtools package in the Integrative Genome
490 Browser (IGV)[39]. ChIP-seq peaks were called by comparing the IP with the Input using
491 Model-based Analysis of ChIP-Seq (MACS2) with the "-p 0.05 -g 1.19e8" option ($P <$
492 $0.05$)[66]. The peaks were annotated using the nearest gene using the Bioconductor and the
493 ChIPpeakAnno packages in the R program, from which we identified 2,011 genes detected
494 in both biological replicates. Enrichment of GO categories of the set of 314 genes overlapping
495 between raindrop- and MS-induced genes for biological processes was determined using
496 BiNGO (http://www.psb.ugent.be/cbd/papers/BiNGO/Home.html)[61]. Sequences of the
497 peaks were extracted from the *Arabidopsis thaliana* genome as FASTA files with Bedtools[67].
498 To identify the candidates of CAMTA3-binding motifs, the FASTA files were subjected to
499 MEME (Multiple EM for Motif Elicitation)-ChIP with the default parameter (-meme-minw
500 6-meme-maxw 10)[68], and a density plot of the distribution of the motifs was generated.

501 **Immunoblot analysis for detection of MPK3 and MPK6 phosphorylation**

502 The adaxial side of leaves from 4-week-old plants was brushed four times or treated with
503 four raindrops, and samples (0.1-0.15 g) were snap-frozen in liquid nitrogen. Total proteins
504 were extracted in protein extraction buffer [50 mM Tris-HCl pH 7.5, 150 mM NaCl, 2 mM
505 DTT, 2.5 mM NaF, 1.5 mM $Na_3VO_4$, 0.5% (w/v) Nonidet P-40, 50 mM β-glycerophosphate,
506 and proteinase inhibitor cocktail] and centrifuged once at 6,000 g, 4°C, for 20 min and twice
507 at 17,000 g, 4°C for 10 min. The supernatant was mixed with SDS sample buffer [50 mM
508 Tris-HCl pH 6.8, 2% (w/v) SDS, 5% (w/v) glycerol, 0.02% (w/v) bromophenol blue, and
509 200 mM DTT] and heated at 70°C for 20 min. The protein samples were subjected to SDS-
510 PAGE electrophoresis and transferred onto a nitrocellulose membrane (GE Healthcare, IL,

511 USA). The membrane was incubated with an anti-phospho-p44/42 MAPK polyclonal
512 antibody (Cell Signalling Technology, MA, USA) (1:1,000 dilution) and goat anti-rabbit
513 IgG(H+L)-HRP secondary antibody (BIO-RAD, CA, USA) (1:2,000 dilution). The bands for
514 MPK3/6 were visualized using chemiluminescence solution mixed 5:1 with ImmunoStar
515 Zeta (FUJIFILM Wako Chemicals, Osaka, Japan) and SuperSignal West Dura Extended
516 Duration Substrate (Thermo Fisher Scientific). The Rubisco bands were stained with
517 Ponceau S (Merck Sharp & Dohme Corp., NJ, USA) as a loading control. The
518 phosphorylation levels of MPK3 and MPK6 were quantified with the blot analysis plug-in in
519 ImageJ (https://imagej.nih.gov/ij/).

520 **Treatment with the calcium ionophore A23187**

521 Twelve-day-old Col-0 seedling was treated with 50 μM calcium ionophore A23187 for 15-,
522 30- and 60 min. Samples were processed for the phosphorylation of MPK3 and MPK6 as
523 described in the "Immunoblot analysis for detection of MPK3 and MPK6 phosphorylation"
524 section. The leaf tissue was stored at -80°C until use.

525 **Promoter-reporter imaging**

526 The 3.0-kbp promoters for *WRKY33* and *CBP60g*, both of which covered the previously
527 analyzed respective regulatory sequences, were amplified from Col-0 genomic DNA by PCR
528 and cloned into the pENTR/D-TOPO vector (Invitrogen). The promoter regions were
529 recombined using Gateway technology into the binary vector pBGYN. The resulting
530 pBGYN-pWRKY33-YFP-NLS and pBGYN-pCBP60g-YFP-NLS vectors were introduced
531 into *Agrobacterium tumefaciens* GV3101 (pMP90) and then into *Arabidopsis* Col-0 plants
532 using the floral dip method. A representative homozygous line was selected for each
533 construct for further detailed analyses.

534 Promoter-reporter imaging was performed using an MA205FA automated
535 stereomicroscope (Leica Microsystems, Wetzlar, Germany) and DFC365FX CCD camera
536 (Leica Microsystems) in 12-bit mode. Chlorophyll autofluorescence and YFP fluorescence
537 were detected through Texas Red (TXR) (excitation 560/40 nm, extinction 610 nm) and YFP
538 (excitation 510/20 nm, extinction 560/40 nm) filters (Leica Microsystems). To image
539 fluorescence emanating from the *WRKY33pro:EYFP-NLS* (Col-0) and *CBP60gpro:EYFP-*
540 *NLS* (Col-0) plants[56], the leaves of 3-week-old *Arabidopsis* plants were brushed 10 times at
541 an interval of 15 min for 2 h or left untreated.

542 **Promoter analysis**

543 The statistical analysis for overrepresented transcriptional regulatory elements across
544 transcriptome datasets described above was calculated using a prediction program as
545 previously reported[32]. The *P* values were calculated using Statistical Motif Analysis in
546 Promoter or Upstream Sequences
547 (https://www.arabidopsis.org/tools/bulk/motiffinder/index.jsp). Figures of promoter motif
548 sequences are generated with WebLogo (https://weblogo.berkeley.edu/logo.cgi).

549 **Real-time $[Ca^{2+}]_{cyt}$ imaging**

550 We used 4-week-old and 3-week-old plants expressing the GFP-based cytosolic $Ca^{2+}$
551 concentration ($[Ca^{2+}]_{cyt}$) indicator GCaMP3[43,44]. To image the fluorescence from the
552 GCaMP3 reporter (in Col-0 and *gl1*) in whole leaves, the adaxial sides of leaves from 4-
553 week-old plants were brushed. To monitor the calcium waves propagating from trichomes, a
554 single trichome from a 2-week-old seedling was flicked with a silver chloride wire. Samples
555 were imaged with a motorized fluorescence stereomicroscope (SMZ-25; Nikon, Tokyo,
556 Japan) equipped with a 1× objective lens (NA = 0.156, P2-SHR PLAN APO; Nikon) and an

557 sCMOS camera (ORCA-Flash 4.0 V2; Hamamatsu Photonics, Shizuoka, Japan) as
558 described[44].

559 **Propidium iodide staining**

560 A stock solution of 10 mM propidium iodide (PI) was prepared with phosphate-buffered
561 saline (PBS). Rosette leaves of 4-week-old Col-0 plants were cut into 5 mm squares, floated
562 in a glass petri dish with 20 μM PI solution, and incubated for 1 h at room temperature.
563 Stained tissues were observed under the all-in-one fluorescence microscope (BZ-X800;
564 KEYENCE CORPORATION, Osaka, Japan) equipped with a 20x objective lens (CFI S Plan
565 Fluor LWD ADM 20XC, Nikon) and TRITC dichroic mirror (excitation 545/25 nm,
566 extinction 605/70 nm) (KEYENCE).

567 **Bacterial infection**

568 MS were applied to the adaxial leaf surface of 4-week-old plants by brushing 4 times at an
569 interval of 15 min for 3 h. Sample leaves were then inoculated by infiltration, using a plastic
570 syringe (Terumo Tuberculin Syringe 1 mL; TERUMO), with *Psm* ES4326 ($OD_{600}$ = 0.001)
571 resuspended in 10 mM $MgCl_2$. Bacterial growth was measured 2 days after inoculation as
572 described previously[69].

573 **Fungal infection**

574 *Alternaria brassicicola* strain Ryo-1 was cultured on 3.9% (w/v) potato dextrose agar plates
575 (PDA; Becton, Dickinson and Company, NJ, USA) for 4-20 days at 28°C in the dark. After
576 incubation of the agar plates for 3-7 days under ultraviolet C light, a conidial suspension of
577 *A. brassicicola* was obtained by mixing with RO water[70]. The adaxial side of leaves from 4-
578 week-old plants was treated with 10 droplets or MS by brushing at an interval of 15 min for
579 3 h, followed by spotting with 5 μL conidia suspension (2 x $10^5$ per mL) of *A. brassicicola*

580 on the adaxial side of leaves. Inoculated plants were placed at 22°C under diurnal conditions
581 (16-h-light/8-h-dark cycles) with 100% relative humidity. The lesion size of fungal infection
582 was measured with ImageJ 3 days after inoculation.

583 **Statistics and reproducibility**

584 GraphPad Prism 9 (GraphPad software, CA, USA) was used for all statistical analyses. Two-
585 sided one-way analysis of variance (one-way ANOVA) or two-way analysis of variance
586 (two-way ANOVA) was used for multiple comparisons. Unless stated otherwise, sample size
587 n represents technical replicates. In RT-qPCR, $n \geq 3$; in bacterial growth assays, $n = 8$; in
588 real-time $[Ca^{2+}]_{cyt}$ imaging assays of *35Spro:GCaMP3* (Col-0) and *35Spro:GCaMP3* (*gl1*),
589 $n = 14$ and 9, respectively; and in fungal disease propagation assays, $n = 29$ (Fig. 2g) and n
590 = 15 (the other figures). All experiments were performed at least three times with similar
591 results (biological replicates). In all graphs, asterisks indicate statistical significance tested
592 by Student's *t* test (two groups) or one/two-way ANOVA (multiple groups).

593 **Reporting summary**

594 Further information on research design is available in the Nature Research Reporting
595 Summary linked to this article.

596 **Date availability**

597 The authors declare that all data supporting the findings of this study are available within this
598 article and its Supplementary Information files. RNA-seq and ChIP-seq data have been
599 deposited in the DDBJ Sequence Read Archive (DRA) at the DNA Data Bank (DDBJ;
600 http://www.ddbj.nig.ac.jp/) through the accession numbers DRA011970, DRA009248 and
601 DRA011123.

602 **References**

603


604 1. Couto, D. & Zipfel, C. Regulation of pattern recognition receptor signalling in plants.
605 *Nat. Rev. Immunol.* **16**, 537-552 (2016).
606 2. Zipfel, C. et al. Bacterial disease resistance in *Arabidopsis* through flagellin
607 perception. *Nature* **428**, 764-767 (2004).
608 3. Chisholm, S. T., Coaker, G., Day, B. & Staskawicz, B. J. Host-microbe interactions:
609 shaping the evolution of the plant immune response. *Cell* **124**, 803-814 (2006).
610 4. Cui, H., Tsuda, K. & Parker, J. E. Effector-triggered immunity: from pathogen
611 perception to robust defense. *Annu. Rev. Plant Biol.* **66**, 487-511 (2015).
612 5. Jones, J. D. & Dangl, J. L. The plant immune system. *Nature* **444**, 323-329 (2006).
613 6. Boudsocq, M. et al. Differential innate immune signalling via Ca(2+) sensor protein
614 kinases. *Nature* **464**, 418-422 (2010).
615 7. Macho, A. P. & Zipfel, C. Plant PRRs and the activation of innate immune signaling.
616 *Mol. Cell* **54**, 263-272 (2014).
617 8. Mwimba, M. et al. Daily humidity oscillation regulates the circadian clock to
618 influence plant physiology. *Nat. Commun.* **9**, 4290 (2018).
619 9. Wang, W. et al. Timing of plant immune responses by a central circadian regulator.
620 *Nature* **470**, 110-114 (2011).
621 10. Zhou, M. et al. Redox rhythm reinforces the circadian clock to gate immune response.
622 *Nature* **523**, 472-476 (2015).
623 11. Madden, L. V. Effects of rain on splash dispersal of fungal pathogens. *CANADIAN J.*
624 *Plant Pathol.* **19**, 225-230 (1997).
625 12. Schwartz, H. F., Otto, K. L. & Gent, D. H. Relation of temperature and rainfall to
626 development of Xanthomonas and Pantoea leaf blights of onion in Colorado. *Plant*
627 *Dis.* **87**, 11-14 (2003).
628 13. Melotto, M., Underwood, W., Koczan, J., Nomura, K. & He, S. Y. Plant stomata
629 function in innate immunity against bacterial invasion. *Cell* **126**, 969-980 (2006).
630 14. Xin, X. F. et al. Bacteria establish an aqueous living space in plants crucial for
631 virulence. *Nature* **539**, 524-529 (2016).
632 15. Braam, J. & Davis, R. W. Rain-, wind-, and touch-induced expression of calmodulin
633 and calmodulin-related genes in Arabidopsis. *Cell* **60**, 357-364 (1990).

634 16. Jaffe, M. J. Thigmomorphogenesis: The response of plant growth and development
635 to mechanical stimulation : With special reference to *Bryonia dioica*. *Planta* **114**, 143-
636 157 (1973).
637 17. Sanyal, D. & Bangerth, F. Stress induced ethylene evolution and its possible
638 relationship to auxin-transport, cytokinin levels, and flower bud induction in shoots
639 of apple seedlings and bearing apple trees. *Plant Growth Regul.* **24**, 124-134 (1998).
640 18. Johnson, K. A., Sistrunk, M. L., Polisensky, D. H. & Braam, J. *Arabidopsis thaliana*
641 responses to mechanical stimulation do not require ETR1 or EIN2. *Plant Physiol.* **116**,
642 643-649 (1998).
643 19. Lange, M. J. & Lange, T. Touch-induced changes in *Arabidopsis* morphology
644 dependent on gibberellin breakdown. *Nat. Plants* **1**, 14025 (2015).
645 20. Van Moerkercke, A. et al. A MYC2/MYC3/MYC4-dependent transcription factor
646 network regulates water spray-responsive gene expression and jasmonate levels. *Proc.*
647 *Natl. Acad. Sci. U S A* **116**, 23345-23356 (2019).
648 21. Li, B., Meng, X., Shan, L. & He, P. Transcriptional regulation of pattern-triggered
649 immunity in plants. *Cell Host Microbe* **19**, 641-650 (2016).
650 22. Pandey, S. P. & Somssich, I. E. The role of WRKY transcription factors in plant
651 immunity. *Plant Physiol.* **150**, 1648-1655 (2009).
652 23. Dong, X., Mindrinos, M., Davis, K. R. & Ausubel, F. M. Induction of Arabidopsis
653 defense genes by virulent and avirulent Pseudomonas syringae strains and by a cloned
654 avirulence gene. *Plant Cell* **3**, 61-72 (1991).
655 24. Fu, Z. Q. & Dong, X. Systemic acquired resistance: turning local infection into global
656 defense. *Annu. Rev. Plant Biol.* **64**, 839-863 (2013).
657 25. Howe, G. A. & Jander, G. Plant immunity to insect herbivores. *Annu. Rev. Plant Biol.*
658 **59**, 41-66 (2008).
659 26. Tena, G., Boudsocq, M. & Sheen, J. Protein kinase signaling networks in plant innate
660 immunity. *Curr. Opin. Plant Biol..* **14**, 519-529 (2011).
661 27. Galletti, R., Ferrari, S. & De Lorenzo, G. Arabidopsis MPK3 and MPK6 play
662 different roles in basal and oligogalacturonide- or flagellin-induced resistance against
663 *Botrytis cinerea*. *Plant Physiol.* **157**, 804-814 (2011).
664 28. Su, J. et al. Active photosynthetic inhibition mediated by MPK3/MPK6 is critical to
665 effector-triggered immunity. *PLoS Biol.* **16**, e2004122 (2018).

666 29. Bouche, N., Scharlat, A., Snedden, W., Bouchez, D. & Fromm, H. A novel family of
667 calmodulin-binding transcription activators in multicellular organisms. *J. Biol. Chem.*
668 **277**, 21851-21861 (2002).
669 30. Doherty, C. J., Van Buskirk, H. A., Myers, S. J. & Thomashow, M. F. Roles for
670 *Arabidopsis* CAMTA transcription factors in cold-regulated gene expression and
671 freezing tolerance. *Plant Cell* **21**, 972-984 (2009).
672 31. Finkler, A., Ashery-Padan, R. & Fromm, H. CAMTAs: calmodulin-binding
673 transcription activators from plants to human. *FEBS Lett.* **581**, 3893-3898 (2007).
674 32. Yamamoto, Y. Y. et al. Identification of plant promoter constituents by analysis of
675 local distribution of short sequences. *BMC Genomics* **8**, 67 (2007).
676 33. Yang, Y. et al. Genome-wide identification of *CAMTA* gene family members in
677 *Medicago truncatula* and their expression during root nodule symbiosis and hormone
678 treatments. *Front. Plant Sci.* **6**, 459 (2015).
679 34. Du, L. et al. Ca(2+)/calmodulin regulates salicylic-acid-mediated plant immunity.
680 *Nature* **457**, 1154-1158 (2009).
681 35. Galon, Y. et al. Calmodulin-binding transcription activator (CAMTA) 3 mediates
682 biotic defense responses in *Arabidopsis*. *FEBS Lett.* **582**, 943-948 (2008).
683 36. Kim, Y. S. et al. CAMTA-mediated regulation of salicylic acid immunity pathway
684 genes in Arabidopsis exposed to low temperature and pathogen infection. *Plant Cell*
685 **29**, 2465-2477 (2017).
686 37. Nie, H. et al. SR1, a calmodulin-binding transcription factor, modulates plant defense
687 and ethylene-induced senescence by directly regulating NDR1 and EIN3. *Plant*
688 *Physiol.* **158**, 1847-1859 (2012).
689 38. Kim, Y., Park, S., Gilmour, S. J. & Thomashow, M. F. Roles of CAMTA transcription
690 factors and salicylic acid in configuring the low-temperature transcriptome and
691 freezing tolerance of Arabidopsis. *Plant J.* **75**, 364-376 (2013).
692 39. Thorvaldsdottir, H., Robinson, J. T. & Mesirov, J. P. Integrative Genomics Viewer
693 (IGV): high-performance genomics data visualization and exploration. *Brief*
694 *Bioinformatics* **14**, 178-192 (2013).
695 40. Gutschick, V. P. Biotic and abiotic consequences of differences in leaf structure. *New*
696 *Phytol.* **143**, 3-18 (2002).
697 41. Wagner, G. J., Wang, E. & Shepherd, R. W. New approaches for studying and
698 exploiting an old protuberance, the plant trichome. *Ann. Bot.* **93**, 3-11 (2004).

42. Zhou, L. H. et al. The Arabidopsis trichome is an active mechanosensory switch. *Plant Cell Environ.* **40**, 611-621 (2017).
43. Tian, L. et al. Imaging neural activity in worms, flies and mice with improved GCaMP calcium indicators. *Nat. Methods* **6**, 875-881 (2009).
44. Toyota, M. et al. Glutamate triggers long-distance, calcium-based plant defense signaling. *Science* **361**, 1112-1115 (2018).
45. Larkin, J. C., Oppenheimer, D. G., Lloyd, A. M., Paparozzi, E. T. & Marks, M. D. Roles of the GLABROUS1 and TRANSPARENT TESTA GLABRA genes in Arabidopsis trichome development. *Plant Cell* **6**, 1065-1076 (1994).
46. Xia, Y. et al. The *glabra1* mutation affects cuticle formation and plant responses to microbes. *Plant Physiol.* **154**, 833-846 (2010).
47. Mao, G. et al. Phosphorylation of a WRKY transcription factor by two pathogen-responsive MAPKs drives phytoalexin biosynthesis in *Arabidopsis*. *Plant Cell* **23**, 1639-1653 (2011).
48. Tsuda, K. & Somssich, I. E. Transcriptional networks in plant immunity. *New Phytol.* **206**, 932-947 (2015).
49. Chehab, E. W., Yao, C., Henderson, Z., Kim, S. & Braam, J. *Arabidopsis* touch-induced morphogenesis is jasmonate mediated and protects against pests. *Curr. Biol.* **22**, 701-706 (2012).
50. Bauer, H. et al. The contribution of bacteria and fungal spores to the organic carbon content of cloud water, precipitation and aerosols. *Atmospheric Research* **64**, 109-119 (2002).
51. Prussin, A. J. 2nd, Marr, L. C. & Bibby, K. J. Challenges of studying viral aerosol metagenomics and communities in comparison with bacterial and fungal aerosols. *FEMS Microbiol. Lett.* **357**, 1-9 (2014).
52. Huynh, T.-P. & Haick, H. Learning from an intelligent mechanosensing system of plants. *Adv. Mater. Technol.* **4**, 1800464 (2019).
53. Scherzer, S., Federle, W., Al-Rasheid, K. A. S. & Hedrich, R. Venus flytrap trigger hairs are micronewton mechano-sensors that can detect small insect prey. *Nat. Plants* **5**, 670-675 (2019).
54. Bacete, L. & Hamann, T. The Role of mechanoperception in plant cell wall integrity maintenance. *Plants (Basel, Switzerland)* **9**, (2020).

731 55. Suda, H. et al. Calcium dynamics during trap closure visualized in transgenic Venus
732 flytrap. *Nat. Plants* **6**, 1219-1224 (2020).
733 56. Betsuyaku, S. et al. Salicylic acid and jasmonic acid pathways are activated in
734 spatially different domains around the infection site during effector-triggered
735 immunity in *Arabidopsis thaliana*. *Plant Cell Physiol.* **59**, 8-16 (2018).
736 57. Murashige, T. & Skoog, F. A revised medium for rapid growth and bio assays with
737 Tobacco tissue cultures. *Physiol. Plant.* **15**, 473-497 (1962).
738 58. Gunn, R. & Kinzer, G. D. The terminal velocity of fall for water droplet in stagnant
739 air. *J. Atmospheric Sci.* **6**, 243-248 (1949).
740 59. Robinson, M. D., McCarthy, D. J. & Smyth, G. K. edgeR: a Bioconductor package
741 for differential expression analysis of digital gene expression data. *Bioinformatics* **26**,
742 139-140 (2010).
743 60. Langmead, B. & Salzberg, S. L. Fast gapped-read alignment with Bowtie 2. *Nat.*
744 *Methods* **9**, 357-359 (2012).
745 61. Maere, S., Heymans, K. & Kuiper, M. BiNGO: a Cytoscape plugin to assess
746 overrepresentation of gene ontology categories in biological networks.
747 *Bioinformatics* **21**, 3448-3449 (2005).
748 62. Denoux, C. et al. Activation of defense response pathways by OGs and flg22 elicitors
749 in *Arabidopsis* seedlings. *Mol. Plant* **1**, 423-445 (2008).
750 63. Matsuura, T., Mori, I. C., Himi, E. & Hirayama, T. Plant hormone profiling in
751 developing seeds of common wheat (*Triticum aestivum L.*). *Breeding Science* **69**, 601-
752 610 (2019).
753 64. Yamaguchi, N. et al. PROTOCOLS: Chromatin immunoprecipitation from
754 Arabidopsis tissues. *The arabidopsis book* **12**, e0170 (2014).
755 65. Li, H. et al. The Sequence Alignment/Map format and SAMtools. *Bioinformatics* **25**,
756 2078-2079 (2009).
757 66. Zhang, Y. et al. Model-based Analysis of ChIP-Seq (MACS). *Genome Biol.* **9**, R137
758 (2008).
759 67. Quinlan, A. R. & Hall, I. M. BEDTools: a flexible suite of utilities for comparing
760 genomic features. *Bioinformatics* **26**, 841-842 (2010).
761 68. Machanick, P. & Bailey, T. L. MEME-ChIP: motif analysis of large DNA datasets.
762 *Bioinformatics* **27**, 1696-1697 (2011).

763 69. Cao, H., Bowling, S. A., Gordon, A. S. & Dong, X. Characterization of an
764 Arabidopsis mutant that is nonresponsive to inducers of systemic acquired resistance.
765 *Plant Cell* **6**, 1583-1592 (1994).
766 70. Hiruma, K. et al. *Arabidopsis ENHANCED DISEASE RESISTANCE 1* is required for
767 pathogen-induced expression of plant defensins in nonhost resistance, and acts
768 through interference of *MYC2*-mediated repressor function. *Plant J.* **67**, 980-992
769 (2011).
770

771 **Acknowledgements**

772 We thank M. F. Thomashow for the seeds of CAMTA3 variants. This work was supported
773 by JSPS KAKENHI Grant Numbers JP23120520, JP25120718, and JP18K19334 (to Y.T.),
774 JP15H05955 (to Y.T. and T.K.), JP19H05363, and JP21H00366 (to M.N.).

775

776 **Author contributions**

777 M.M., M.N., S.H.S., and Y.T. designed the research. M.M. and T.I. established the artificial
778 rain device. M.M. optimized the protocols for artificial raindrop and brush treatment. M.M.
779 and M.N. constructed the Illumina sequencing libraries for RNA-seq and ChIP-seq. T.S.
780 performed RNA-seq and analysis. M.N. performed the ChIP-seq and analysis of CAMTA3.
781 T.M. and I.M. performed the quantification of phytohormones. M.M., Y.H., and T.K.
782 performed the detection of MPK3 and MPK6 phosphorylation. Y.A. and M.T. generated
783 *35Spro*:*GCaMP3* (*gl1*) plants, and M.N., M.T., and Y.A. visualized real-time $[Ca^{2+}]_{cyt}$. M.I.
784 and S.B. generated the transgenic lines *WRKY33pro:EYFP-NLS* (Col-0) and
785 *CBP60gpro:EYFP-NLS* (Col-0). M.M., M.I., and S.B. performed promoter-reporter imaging.
786 M.N. and M.M. performed the rest of the experiments. M.M., M.N., S.H.S., and Y.T. wrote
787 the manuscript with input from all authors.

788

## Competing interests

The authors declare no competing interests.

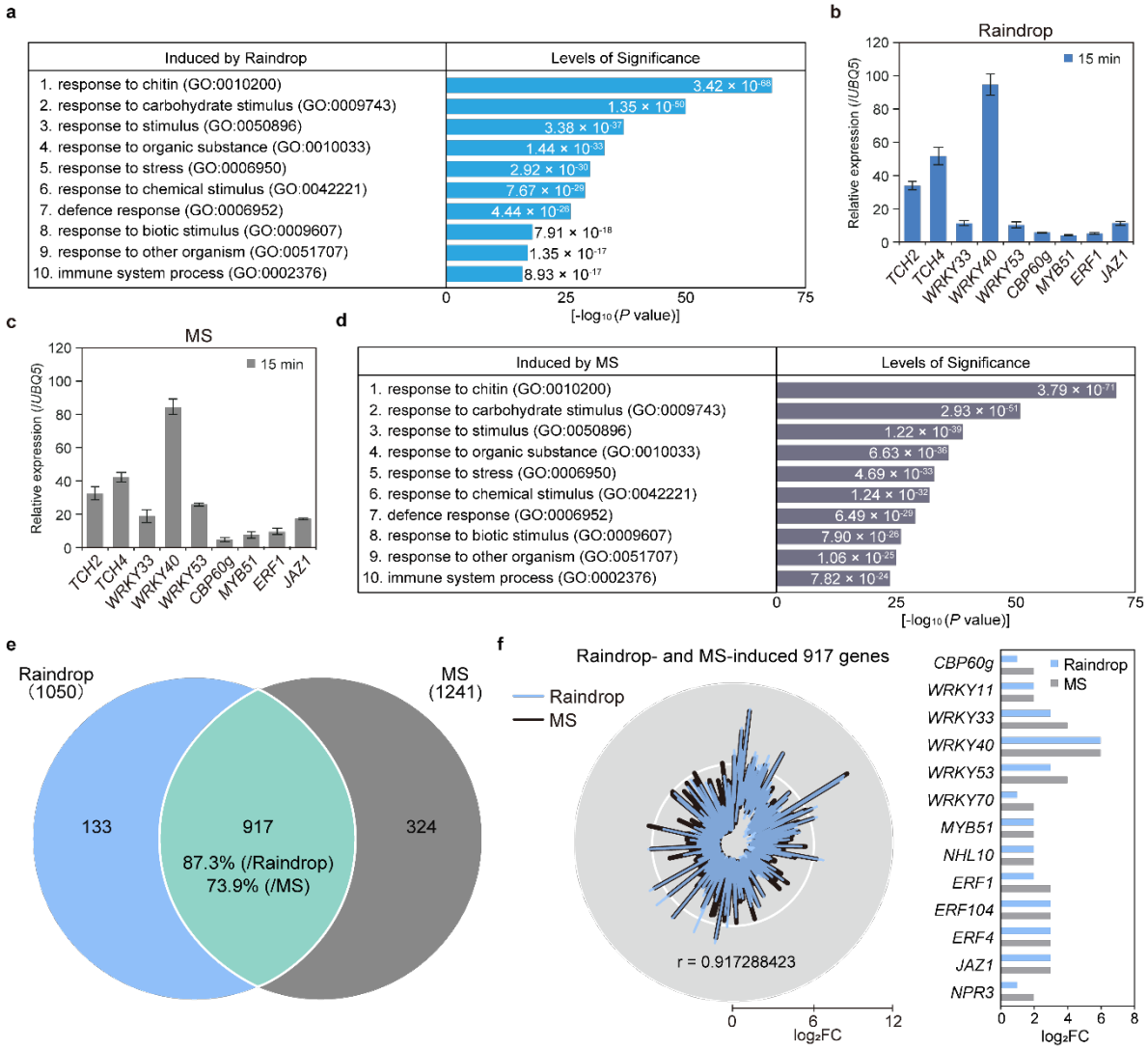


**Fig. 1 | Raindrop-induced gene expression highly correlates with mechanical stimuli (MS)-induced gene expression in *Arabidopsis*.** **a** Enriched Gene Ontology (GO) categories of 1,050 raindrop (10 droplets)-induced genes in the wild type (Col-0). The top 10 categories are shown in ascending order of *P* values. **b**, **c** Transcript levels of MS-induced and defence-related genes in 4-week-old Col-0 plants 15 min after being treated with 10 falling droplets (raindrop, **b**) or 1 brushing (MS, **c**), determined by RT-qPCR and normalized to *UBIQUITIN 5* (*UBQ5*). Data are presented as mean ± SD. **d** Enriched GO categories of 1,241 MS (1 brushing)-induced genes in Col-0. The top 10 categories are shown in ascending order of *P* values. **e** Venn diagram of the overlap between transcriptome datasets from raindrop- and MS-induced genes ($P < 0.05$). **f** Radar chart of intensity compared with mock ($\log_2$FC) and

803 Pearson correlation coefficient (r = 0.917288423) of 917 raindrop- and MS-induced genes
804 (left). Intensities of major immune regulator genes induced by raindrops and MS in RNA-
805 seq analysis ($log_2FC$) (right).
806

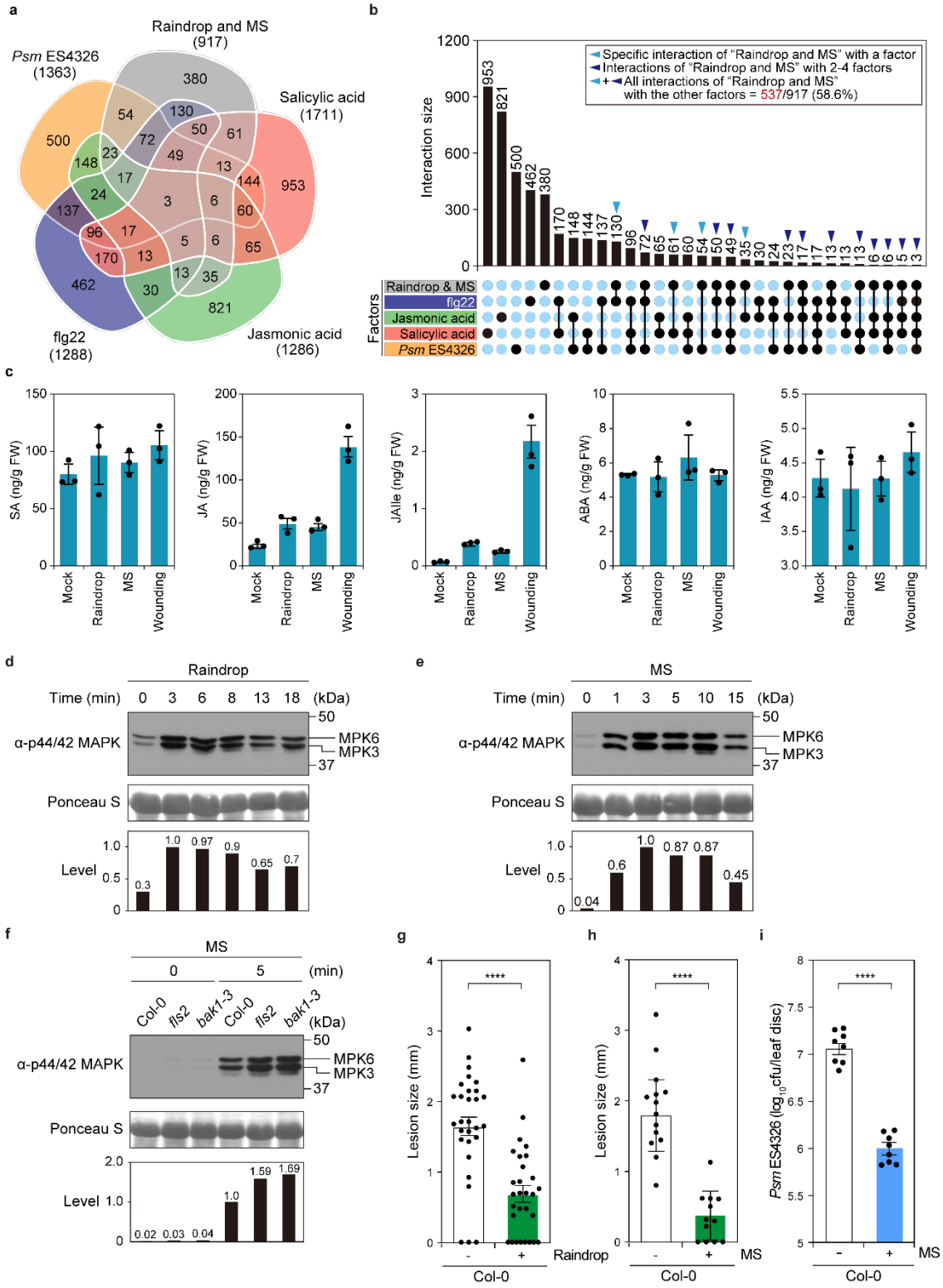
a
Raindrop and MS (917)
Psm ES4326 (1363)
Salicylic acid (1711)
flg22 (1288)
Jasmonic acid (1286)
b
Specific interaction of "Raindrop and MS" with a factor
Interactions of "Raindrop and MS" with 2-4 factors
All interactions of "Raindrop and MS" with the other factors = 537/917 (58.6%)
Interaction size
Factors
Raindrop & MS
flg22
Jasmonic acid
Salicylic acid
Psm ES4326
c
SA (ng/g FW)
JA (ng/g FW)
JAIle (ng/g FW)
ABA (ng/g FW)
IAA (ng/g FW)
Mock
Raindrop
MS
Wounding
d
Raindrop
Time (min)
(kDa)
α-p44/42 MAPK
MPK6
MPK3
Ponceau S
Level
e
MS
f
Col-0
fls2
bak1-3
(min)
g
h
i
Lesion size (mm)
Psm ES4326 (log10 cfu/leaf disc)
****
Raindrop
MS
Col-0

807

808 **Fig. 2 | Raindrop-induced mechanosensation triggers defence responses in *Arabidopsis.***
809 **a**, **b** Venn diagram (**a**) and the upset plot (**b**) between 917 raindrop- and MS-induced genes
810 and transcriptome datasets obtained from salicylic acid (SA), jasmonic acid (JA), and flg22
811 (PAMP) treatment and *Psm* ES4326 infection ($P < 0.05$). Overlap with raindrop- and MS-
812 induced genes: SA, 21%, 193/917 genes; JA, 11.8%, 108/917 genes; flg22, 37%, 339/917
813 genes; *Psm* ES4326, 25.8%, 237/917 genes; any of the four factors, 58.6%, 537/917 genes.
814 **c** Fresh weight (ng/g) of plant hormones SA, JA, JA-isoleucine (JA-Ile), abscisic acid (ABA),
815 and indole-3-acetic acid (IAA) 5 min after 10 falling droplets (raindrop), 1 brushing (MS),
816 and cutting (wounding). **d**, **e** Raindrop (4 droplets)- (**d**) and MS (4 brushing)-induced (**e**)
817 MAPK activation in Col-0. Total proteins were extracted from 4-week-old plants treated with
818 raindrops and detected by immunoblot analysis with anti-p44/42 MAPK antibodies. Relative
819 phosphorylation levels are shown below each blot. **f** MS-induced MAPK activation in Col-
820 0, *fls2*, and *bak1-3*. Total proteins were extracted from 4-week-old plants after 5 min of MS
821 treatment (1 brushing) and detected by immunoblot analysis with anti-p44/42 MAPK
822 antibodies. Relative phosphorylation levels are shown below each blot. **g, h** Disease
823 progression of *Alternaria brassicicola* in Col-0 leaves 3 days after inoculation with (+) or
824 without (–) raindrop (10 droplets) pretreatment (**g**) or with (+) or without (–) MS (4 brushing)
825 pretreatment (**h**). Error bars represent SE. Asterisks indicate significant difference (one-way
826 ANOVA; ****$P < 0.0001$). **i** Growth of *Psm* ES4326 in Col-0 leaves 2 days after inoculation
827 with (+) or without (–) MS (4 brushing) pretreatment. An outline of the experiment is
828 provided at left. Error bars represent SE. Asterisks indicates significant difference (one-way
829 ANOVA; ****$P < 0.0001$). Cfu, colony-forming units.
830

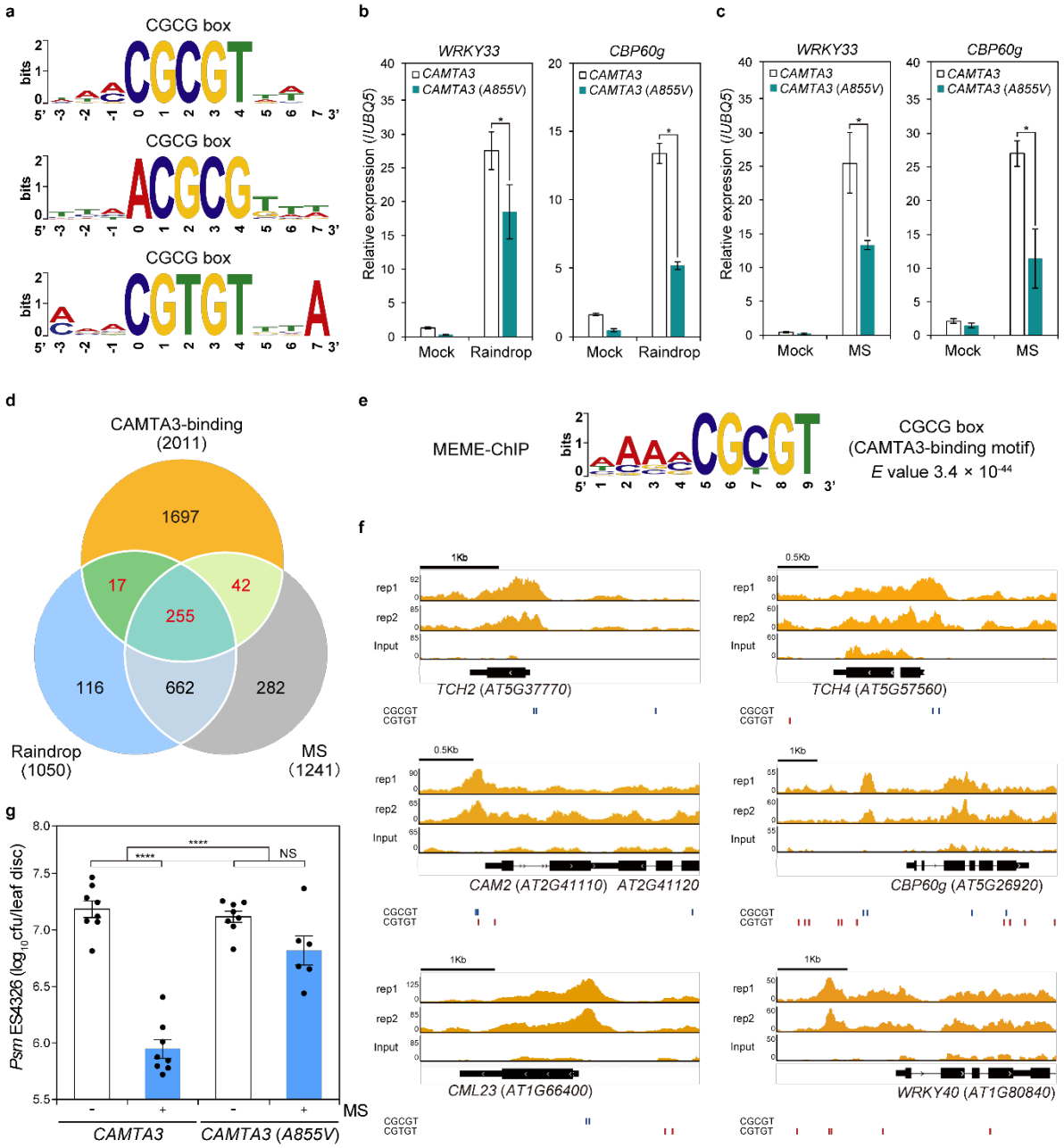


**Fig. 3 | MS-induced genes are regulated by CAMTA3. a** Promoter analysis of the top 300 (among 917 genes) raindrop- and MS-induced genes in terms of expression levels revealed that the CAMTA-binding CGCG box [CGC(/T)GT] were overrepresented among these genes. **b**, **c** Transcript levels of *WRKY33* and *CBP60g* in 4-week-old *camta2 camta3 CAMTA3pro:CAMTA3-GFP* (*CAMTA3*) and *camta2 camta3 CAMTA3pro:CAMTA3*$^{A855V}$-*GFP* [*CAMTA3*(*A855V*)] plants 15 min after the plants were treated with 1 falling droplet (**b**)

838 or brushed 4 times (**c**), determined by RT-qPCR and normalized to *UBQ5* transcript levels.
839 Data are presented as mean ± SD. **d** Venn diagram depicting the overlap between genes with
840 CAMTA3-binding sites in their promoters, as determined by ChIP-seq, and raindrop- and
841 MS-induced genes as determined by RNA-seq. A total of 314 genes, shown in red, were
842 identified as CAMTA3-target genes. **e** The CGCG box was identified as an overrepresented
843 motif among the sequence peaks of 314 genes by MEME-ChIP. **f** Localization of CAMTA3
844 on the promoters of the MS-induced genes *TCH2*, *TCH4*, *CAM2*, *CBP60g*, *CML23*, and
845 *WRKY40*, as representative of the 314 genes shown in (**d**). Blue and red lines indicate
846 CGCGT and CGTGT, respectively. **g** Growth of *Psm* ES4326 in *camta2 camta3*
847 *CAMTA3pro:CAMTA3-GFP* (*CAMTA3*) and *camta2 camta3 CAMTA3pro:CAMTA3*$^{A855V}$-
848 *GFP* [*CAMTA3*(*A855V*)] plants 2 days after inoculation with (+) or without (–) MS (4
849 brushing) pretreatment. Error bars represent SE. Asterisks indicate significant difference
850 (one- and two-way ANOVA; ****$P < 0.0001$). Cfu, colony-forming units. NS, not significant.
851

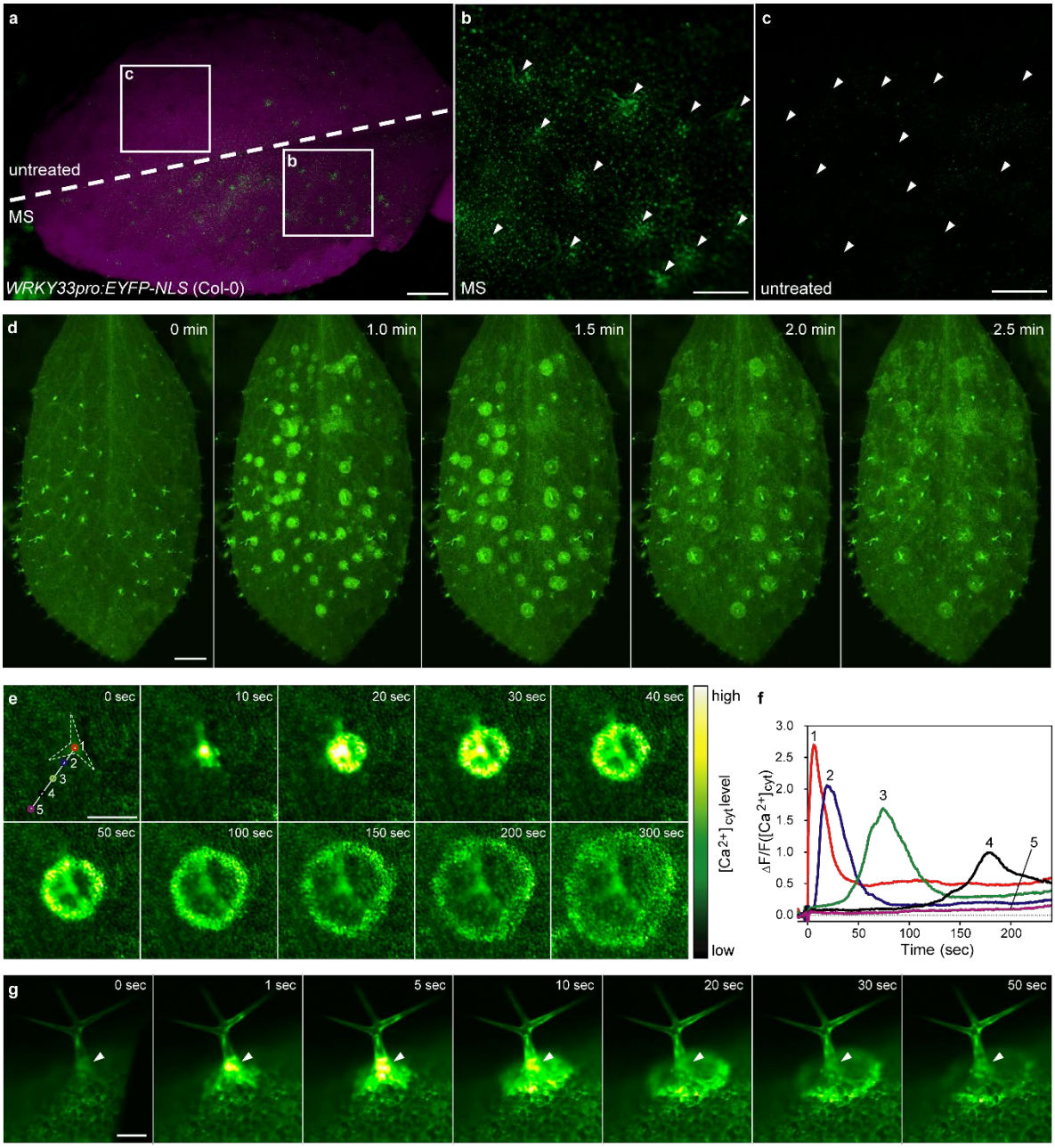


**Fig. 4 | Trichomes initiate intercellular calcium waves. a–c** YFP fluorescence in a whole leaf from *WRKY33pro:EYFP-NLS* (Col-0) with (MS, bottom half) or without brushing (untreated, top half) (**a**), along with zoomed-in views of brushed (**b**) and untreated (**c**) areas. Arrowheads indicate trichomes (**b, c**). Scale bars, 0.5 mm (**a**), 0.3 mm (**b**, **c**). **d** $Ca^{2+}$ imaging using *35Spro:GCaMP3* (Col-0). The leaf surface of a 4-week-old plant was treated with MS by brushing. MS-induced intercellular calcium waves propagated concentrically from

859 trichomes. Scale bar, 1.0 mm. See also Supplementary Video 1. **e** $Ca^{2+}$ imaging using
860 *35Spro:GCaMP3* (Col-0). A single trichome from a 2-week-old seedling was flicked with a
861 silver chloride wire. MS-induced intercellular calcium waves propagated concentrically from
862 the trichome (dashed outline). Scale bar, 0.2 mm. See also Supplementary Video 2. **f** $[Ca^{2+}]_{cyt}$
863 changes at sites indicated by numbers in (**e**). **g** Side view of a trichome whose neck was
864 flicked with a silver chloride wire. MS-induced intercellular $Ca^{2+}$ influx was transiently
865 observed in the trichome base (arrowheads) followed by the formation of circular waves.
866 Scale bar, 0.1 mm. See also Supplementary Video 3.
867

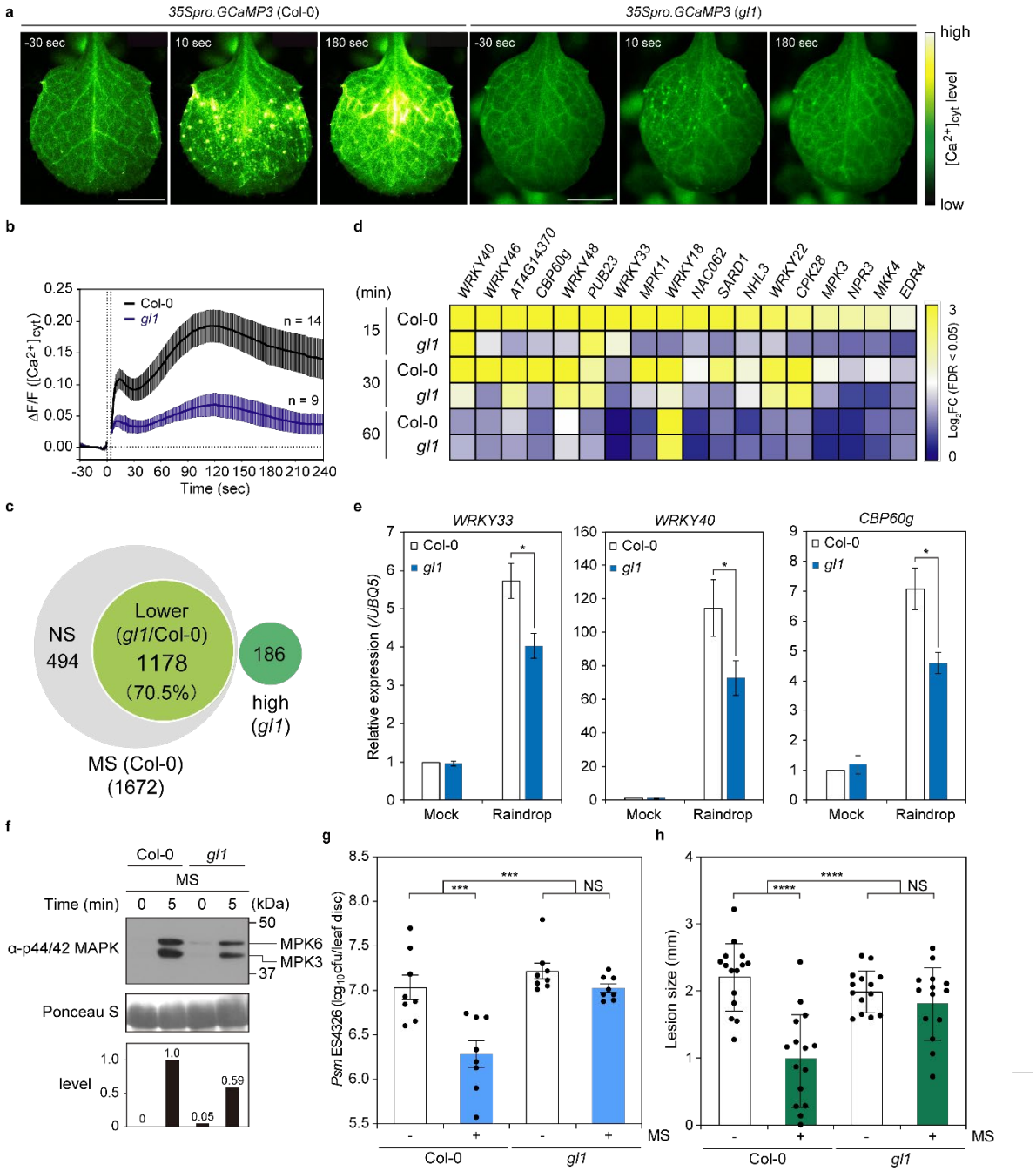


**Fig. 5 | Trichomes are mechanosensory cells. a** $Ca^{2+}$ imaging using *35Spro:GCaMP3* (Col-0) and *35Spro:GCaMP3* (*gl1*). Leaf surfaces were exposed to MS by brushing. MS-induced calcium waves were compromised in the *gl1* mutant. See also Supplementary Videos 4 and 5. Scale bars, 0.5 mm. **b** $[Ca^{2+}]_{cyt}$ signature of (**a**). **c** Venn diagram of transcriptome datasets

873 for MS-induced genes in Col-0 and *gl1* ($P < 0.05$). NS, not significant. Lower, fold change
874 (FC) (*gl1*)/FC (Col-0) < 0.5. High, MS (*gl1*)/Mock (*gl1*), $\log_2$FC ≥ 1 in *gl1*. $P < 0.05$. **d**
875 Heatmap of differentially expressed defence-related genes obtained from transcriptome
876 datasets from Col-0 and *gl1* plants treated with MS (4 brushing). **e** Transcript levels of
877 *WRKY33*, *WRKY40*, and *CBP60g* in 4-week-old Col-0 and *gl1* plants 15 min after treatment
878 with 4 falling droplets, determined using RT-qPCR and normalized to *UBQ5*. Data are
879 presented as mean ± SD. Asterisks indicate significant difference (one- and two-way
880 ANOVA; *$P < 0.05$). **f** MS-induced MAPK activation in Col-0 and *gl1*. Total proteins were
881 extracted from 4-week-old leaves 5 min after MS treatment and detected by immunoblot
882 analysis with anti-p44/42 MAPK antibodies. Relative phosphorylation levels are shown
883 below each blot. **g** Growth of *Psm* ES4326 in Col-0 and *gl1* leaves 2 days after inoculation
884 with (+) or without (–) MS (4 brushing) pretreatment. Error bars represent SE. Asterisks
885 indicate significant difference (one- and two-way ANOVA; ***$P < 0.001$). Cfu, colony-
886 forming units. NS, not significant. **h** Disease progression of *Alternaria brassicicola* in Col-0
887 and *gl1* leaves 3 days after inoculation with (+) or without (–) MS (4 brushing) pretreatment.
888 Error bars represent SE. Asterisks indicate significant difference (one- and two-way ANOVA;
889 ****$P < 0.0001$). NS, not significant.
890

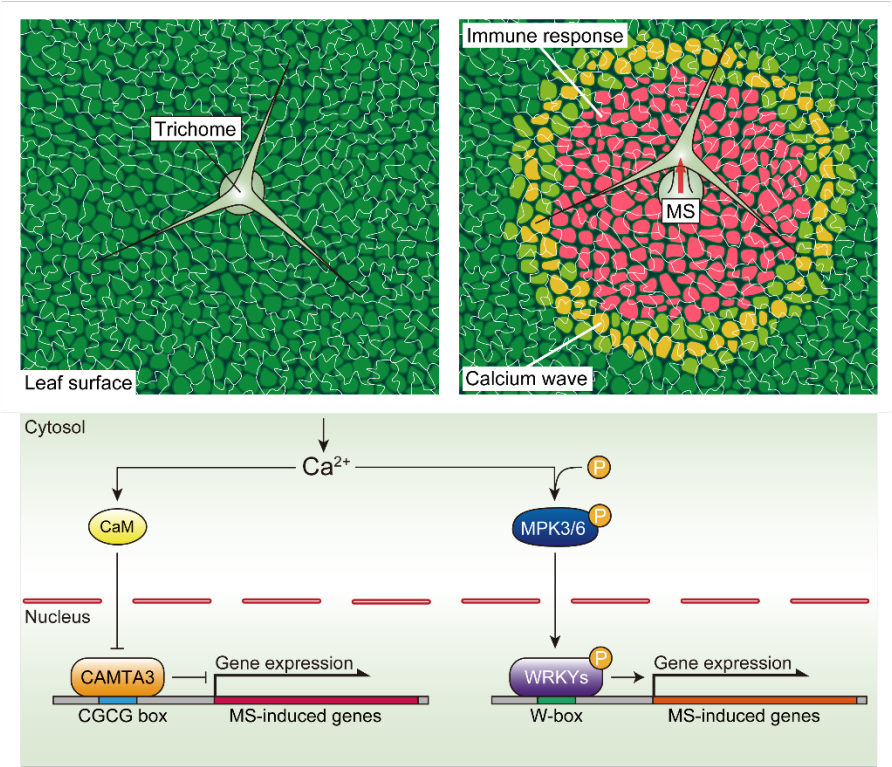


**Fig. 6 | Trichomes activate broad-spectrum disease resistance.** Model showing how trichomes directly sense the mechanical impact of raindrops as an emergency signal in anticipation of possible infections. Mechanosensory trichome cells initiate intercellular calcium waves in response to MS. $[Ca^{2+}]_{cyt}$ initiates the de-repression of $Ca^{2+}$/CaM-dependent CAMTA3 and activates the phosphorylation of MPK3 and MPK6, thereby inducing WRKY-dependent transcription.